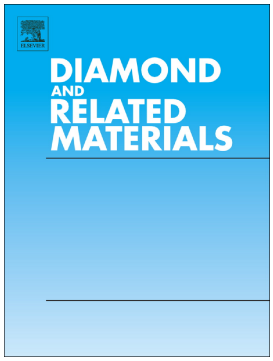

Diamond-EuF3 nanocomposites with bright orange photoluminescence

V.S. Sedov, S.V. Kuznetsov, V.G. Ralchenko, M.N. Mayakova, V.S. Krivobok, S.S. Savin, K.P. Zhuravlev, A.K. Martyanov, I.D. Romanishkin, A.A. Khomich, P.P. Fedorov, V.I. Konov

PII: S0925-9635(16)30526-X
DOI: doi: 10.1016/j.diamond.2016.12.022
Reference: DIAMAT 6789

To appear in: *Diamond & Related Materials*

Received date: 26 September 2016
Revised date: 21 October 2016
Accepted date: 31 December 2016

Please cite this article as: V.S. Sedov, S.V. Kuznetsov, V.G. Ralchenko, M.N. Mayakova, V.S. Krivobok, S.S. Savin, K.P. Zhuravlev, A.K. Martyanov, I.D. Romanishkin, A.A. Khomich, P.P. Fedorov, V.I. Konov , Diamond-EuF3 nanocomposites with bright orange photoluminescence. The address for the corresponding author was captured as affiliation for all authors. Please check if appropriate. Diamat(2016), doi: 10.1016/j.diamond.2016.12.022

Diamond-EuF_3 Nanocomposites with Bright Orange Photoluminescence

V. S. Sedov [a,b,*], S. V. Kuznetsov [a], V. G. Ralchenko [c,a,b], M. N. Mayakova [a], V.S. Krivobok [d], S. S. Savin [e], K. P. Zhuravlev [f], A. K. Martyanov [a], I. D. Romanishkin [a], A. A. Khomich [f], P. P. Fedorov [a], V. I. Konov [a,b]

[a] *General Physics Institute of RAS, Vavilov str. 38, Moscow 119991, Russia*

[b] *National Research Nuclear University MEPhI, Moscow 115409, Russia*

[c] *Harbin Institute of Technology, 92 Xidazhi Str., Harbin 150001, P.R. China*

[d] *Lebedev Physical Institute of RAS, Leninsky Av. 53, Moscow 119991, Russia*

[e] *Moscow Technological University, Moscow 119454, Russia*

[f] *Institute of Radio Engineering and Electronics RAS, Fryazino 141190, Russia*

Abstract: We report the manufacturing of a novel diamond – rare-earth (RE) composite material with EuF_3 nanoparticles (NP) embedded in the synthesized microcrystalline diamond films that show strong photoluminescence in the orange part of the visible spectrum. Synthesis of the aforementioned composite includes placement of EuF_3 NP on the diamond substrate and subsequent coating of them with an additional polycrystalline diamond layer grown by microwave plasma chemical vapor deposition (CVD). The produced composite films exhibit high intensity localized photoluminescence (PL) at 612 nm with the decay time of 0.34 ms, which is generated by the EuF_3 particles buried within a very stable transparent diamond matrix. The proposed synthetic approach is quite versatile, as it allows preparation of the luminescent diamond - RE particles nanocomposites of different sizes and natures which perform well over a broad range of the visible spectrum.

Keywords: *diamond film, photoluminescence, rare earths, europium fluoride*

1. Introduction

Diamond nanophotonics is an area of modern materials science of increasing interest. This field has applications in quantum information technologies [1-5], optical biomarkers [6], and scintillators (X-ray beam monitors) [7,8]. Extensive efforts in this field are focused on the impurity-related color centers in diamond (e.g., nitrogen-vacancy (NV) [9], silicon-vacancy (SiV) [10], germanium-vacancy (GeV) [11,12], chromium- or nickel-related defects [13], etc.). Such color centers typically show narrow (a few nanometers at room temperature) zero phonon lines (ZPL) in photoluminescence (PL) spectra and short PL decay times on the order of

nanoseconds. These color centers can be easily produced by ion implantation in diamond [14] or by chemical vapor deposition (CVD) with *in situ* doping [10, 15]. The known PL properties of the impurity-vacancy centers are quite suitable for engineering of single photon emitters, and the search for new and better PL sources in a diamond matrix is still an ongoing activity. The goal of such studies is to extend the spectral range and increase the decay time and efficiency of diamond-based PL sources. In particular, the PL emission could be further improved using rare-earth (RE) ions, which are known for their higher quantum efficiency and longer PL decay times in the millisecond range. The latter assumption is based on the well-established use of the RE-doped phosphors in white light-emitting devices [17, 18], plasma display panels, field emission displays, solar cells [16], X-ray scintillators [19, 20], etc. Composite luminescent materials with rare-earth fluoride nanoparticles incorporated into oxide glass matrices are also widely implemented [21].

The ideas presented above suggest that the promising combination of chemical stability and lack of diamond cytotoxicity with the unique optical properties of rare-earth ions could be crucially important for the development of RE-containing diamond materials, which can be successfully utilized as brighter bio-markers [22, 23] and X-ray imagers [7,24]. However, the direct incorporation of the large RE ions in the diamond crystal lattice (the densest among solid materials) is very difficult from the technical point of view.

Recently, Magyar et al. [25] reported the first such attempt to introduce RE atoms into a diamond lattice by doping diamond single crystals with europium (Eu^{3+}) organic complex. The authors attached via multistep chemical process Eu(III) tri-(2,6-pyridine dicarboxylic acid) complex (EuDPA) to the polymer layer, assembled on the diamond substrate and then proceeded with diamond deposition to cover the Eu-containing molecules with an outer diamond layer. The obtained material exhibited Eu fluorescence with typical intensive line(s) at 612 nm, but Eu/diamond fluorescence was different than that of the precursor EuDPA complex, with the strongest precursor singlet peak $^5D_0 \rightarrow {}^7F_2$ becoming a multiplet, and broadening and/or splitting of $^5D_0 \rightarrow {}^7F_1$ and $^5D_0 \rightarrow {}^7F_4$ transitions also appearing in the PL spectra.

Our paper describes an alternative approach to incorporate RE elements in diamond by imbedding europium fluoride EuF_3 nanoparticles (NP) in chemical vapor deposition-grown diamond film. Thus, we prepared a composite with the mechanically strong and chemically transparent inert matrix, having the properties inherent to diamond, while retaining the excellent PL properties of EuF_3 particles. Our method allows the manufacture of such diamond-based composites not only just with the one rare earth element, but also with the mixture of several RE metals, in order to fine-tune the PL emission spectrum range.

2. Experimental

Europium trifluoride (EuF_3) has been chosen as the primary object for our studies because of its non-toxic and moisture-resistant nature in comparison with other RE chalcogenides, iodides, bromides, and chlorides, which have a short phonon spectrum. Also, EuF_3 possesses the higher isomorphic capacity and lower phonon energy than RE oxides. EuF_3 exists in two polymorphs: a higher temperature hexagonal tysonite-type α-modification, and a lower temperature orthorhombic β-YF_3 modification [26]. Hexagonal tysonite-type europium (III) fluoride (EuF_3) nanopowders were synthesized by their precipitation from 99.99 wt. % pure 0.2 M aqueous europium nitrate (LANHIT®) and 99.9 wt. % pure 5 vol. % hydrofluoric acid (Chimmed) utilized as the raw materials without any additional purification. The europium nitrate solution was added dropwise to hydrofluoric acid under vigorous stirring at room temperature [27,28].

The formed suspension was separated from the liquid phase by decanting after settling. Then, the precipitate was washed with double-distilled water and dried at 45°C. X-ray diffraction analysis of EuF_3 powder was performed using a Bruker D8 diffractometer (CuK_α radiation). The lattice parameters and the sizes of the coherent scattering domains (D) were calculated using the TOPAS software. A typical X-ray diffraction (XRD) pattern of the synthesized single-phase EuF_3 nanopowder with hexagonal tysonite structure (P-3c1 space symmetry group; a = 6.9191(1), c = 7.0967(1) Å lattice parameters; coherent scattering domain size is about 37 nm; Fig. 1a) is in complete agreement with literature data (JCPDS card 32-0373); no other crystalline phase has been detected. It is worth mentioning that the preparation of the non-equilibrium higher temperature phase at room temperature is a quite common phenomenon in nanotechnology [29].

Samples of an aqueous 0.1wt. % EuF_3 particle slurry was prepared by ultrasonication for 15 min. The particle size distribution in the slurries was measured by the dynamic light scattering (DLS) method using Photocor Complex DLS spectrometer with He-Ne laser as the laser source. The size of separate nanoparticles was measured at 100-400 nm (mode size 220 nm), while a smaller number of larger (600 – 2000 nm) agglomerates were also detected (Fig. 1b).

The scheme for diamond-EuF_3 composite preparation is shown in Fig. 2. At the beginning, the 20 × 20 × 0.5 mm^3 polished (100) single crystal Si wafers, used as the substrates, were seeded with detonation nanodiamonds (average size about 5 nm) in a water-based slurry. Then, ~1.2 μm thick primary microcrystalline diamond film was grown using a microwave plasma chemical vapor deposition (CVD) system ARDIS-100 (2.45 GHz; total gas flow rate =

500 sccm of 5% CH_4/H_2 mixture, 70 Torr pressure, 3.6 kW microwave power, deposition time 40 minutes). The substrate temperature, as measured by two-color Micron M770 pyrometer, was maintained at 800 ^oC. The deposition rate was approximately 1.8 μm/hour, as measured by laser interferometry *in situ* [30].

Formed diamond film was seeded with the EuF_3 NP from an aqueous slurry (0.1 wt% EuF_3) using a spin-coating technique (1 EuF_3 particle per 10 μm^2). We also used the seeding with EuF_3 particles by direct ultrasonic treatment of the substrates in slurries. This method is common for seeding the substrate with a nanodiamond grit to enhance diamond nucleation density. It was quite effective for EuF_3 seeding as well, but in all further experiments only spin-coating seeding was employed. In the next step, additional diamond deposition was continued in order to add the second ~1.2 μm thick microcrystalline diamond layer.

The structure of EuF_3 particles and diamond films was examined with Tescan MIRA3 scanning electron microscope (SEM). The energy-dispersive X-ray spectroscopy (EDX) module was used to detect Eu atoms. Scanning electron microscope study of the synthesized EuF_3 (Fig. 3a) revealed disk-shaped agglomerates (~100 nm thick, and 300 nm in diameter) consisting of ~40 nm primary NPs. The latter value of primary NP size is in excellent agreement with the size of coherent scattering domains (~37 nm) assessed from the XRD data with the use of the Scherrer equation. One such primary EuF_3 particle, seeded on a pre-deposited diamond film with grain size ~400 nm, is shown in Fig.3b. After repeated diamond deposition for 40 minutes, EuF_3 NPs were completely overgrown, and the diamond grain size has been enlarged up to about 1 μm (Fig. 3c). It is worth noting that the used RE fluoride preparation method for synthesizing europium (tri)fluoride nanoparticles allows reduction of the initial RE particle size down to several tens of nanometers if necessary (as has been reported, for example, for LaF_3:Yb:Er [28, 29, 31]).

The position of EuF_3 particles inside the diamond film(s) can be easily identified in the SEM image of the sample's fractured surface (Fig. 3d): the first diamond layer had a columnar structure with continuously increasing grain size, having a fine-grained layer with encapsulated EuF_3 NPs, followed by the 2nd diamond layer on the top. Zoomed images of areas between the two diamond layers reveals individual particles with size of the order of 50 nm, which can be associated with fragmented EuF_3 agglomerates (presumably, the fragmentation was caused by hydrogen etching of thin bridges between elementary EuF_3 nanoparticles). Energy-dispersive X-ray spectroscopy (EDX) of the same cross-section clearly showed a strong Eu signal in the

central region of the film (Fig. 3e), additionally confirming the incorporation of EuF_3 NP in diamond bulk.

Raman spectroscopy and photoluminescence spectra were recorded with LABRAM HR-800 spectrometer equipped with a diode-pumped solid-state laser (λ = 473 nm; the laser beam was focused within ~1 μm spot on the sample surface). Photoluminescence kinetic was analyzed with a laboratory-built system with time-resolved photon counting and direct photocurrent measurements [32]. PL was excited by the radiation of a pulsed diode laser (λ=405 nm) generating a periodic train of 2.5ms -long rectangular light pulses with a pulse energy of 100 μJ at a repetition rate of 20 Hz. Spreading of a rectangular pulse near its edges was no more than 5 ns. The excitation laser beam was focused into a 0.3mm spot on the sample surface. PL signal was analyzed by grating spectrograph equipped with Hamamatsu (H10330B) photomultiplier module.

The typical PL spectrum (550-725 nm) for the freshly-prepared EuF_3 nanopowder (Fig. 4a) contains five lines associated with $^5D_0$-^7F_j transitions (j = 0-4) with the $^5D_0 \rightarrow {}^7F_1$ magnetic-dipole transition dominating. The intensity of the hypersensitive electric-dipole transition $^5D_0 \rightarrow {}^7F_2$, which is very sensitive to the local environment, is notably lower, and the latter suggests a high symmetry of the crystal field for Eu^{3+} ions [33].

3. Results and discussion

The PL spectrum for the embedded EuF_3 NPs is distinctly different from the corresponding starting EuF_3 on the diamond nano-powder spectrum (Fig. 4b). The only common Eu-related feature in these spectra is the narrow line at 611.6 nm which corresponds to the $^5D_0 \rightarrow {}^7F_2$ transition. The pre-deposited diamond film showed no peak at this wavelength (Fig. 4b; bottom spectrum). Another line at 630 nm belongs to a defect of unknown nature related to the CVD diamond [34] and unrelated to EuF_3, for it is also present in the pre-deposited diamond film. The 611.6 nm PL line in the composite is very narrow, with its full width at its half magnitude (FWHM) at only approximately 1.6 nm (Fig. 4c), i.e., far less than for the other Eu-based materials [35, 36]. The 611.6 nm line demonstrates a high intensity, however, the direct comparison of its intensity with that for virgin (uncoated) EuF_3 NPs was difficult as this procedure would require the presence of identical the EuF_3 masses within the probed area of two samples. The two weak peaks at longer wavelengths, λ= 614.3 nm and 624.0 nm, also correspond to the $^5D_0$ - $^7F_2$ transition, but they are much less intense. Also, strongly damped, yet visible, are the lines for the $^5D_0$ - $^7F_1$ transition. Thus, the domination of $^5D_0$-$^7F_2$ transition in the imbedded EuF_3 particles suggests that the symmetry of the local environment around the Eu was

lowered compared to that in the isolated NPs. A similar effect has been observed by Magyar et al. [25] for the cathodoluminescence of Eu defects in nanodiamonds: an intense and broad 612 nm line (FWHM ~20 nm) along with strongly-damped lines corresponding to the other transitions.

In our experiments, apparently, changes in the Eu ion environment have occurred at the boundaries of EuF_3 NPs due to their interaction with carbon atoms. However, since only a minority of all Eu atoms were located at these boundaries, the latter factor alone is unlikely to be responsible for the observed PL spectrum modification. Diamond deposition occurred in an essentially hydrogen-rich plasma in the presence of active atomic hydrogen, so EuF_3 reaction with hydrogen at higher temperature might have resulted in the formation of intermediate-ordered phases such as hexagonal $EuF_{2.40}$ (JCPDS card 26-0626) or tetragonal $EuF_{2.25}$ (JCPDS card 26-0625), or via a polymorphic transformation to low symmetry orthorhombic EuF_3 (JCPDS card 33-0542), thus, lowering the higher original site symmetry of Eu atoms (such transformations of rare-earth fluorides are well known [37,38]). Another reason for the appearance of asymmetry in the inner coordination sphere of Eu atoms may be a biaxial thermal compressive stress in the diamond film (according to our estimate, ~0.25 GPa) due to a mismatch between the thermal expansion coefficients (TEC) for diamond (0.8×10^{-6} K^{-1} at room temperature) and the silicon substrate, resulting in a stress in the encapsulated EuF_3 particles. Also, the thermal stress in EuF_3 particles might originate from a mismatch in the TECs for diamond and fluoride. The mean TEC for the hexagonal europium fluoride is rather high $\sim7\times10^{-5}$ K^{-1} [39] to generate the significant stress in imbedded particle.

The features of the Raman spectra for the diamond films (Fig. 4d) include a narrow (FWHM ~10 cm^{-1}) diamond peak at about 1334 cm^{-1}, broad D- and G-lines from sp^2-bonded amorphous carbon (a-C) at 1350 cm^{-1} and 1580 cm^{-1}, respectively, and the lines at 1140 cm^{-1} and 1450 cm^{-1} corresponding to *trans*-polyacetylene (t-PA) [40]. The a-C and t-PA components are located at hydrogen-tethered grain boundaries, including EuF_3-diamond interfaces. We expect that the fluoride-diamond interface could be more regular/ordered if EuF_3 NPs would be embedded in single crystal diamond compared to the polycrystalline specimens described in the present paper. The experiments on the preparation of such composites are in progress now.

Photoluminescence kinetic was analyzed with a laboratory-built system with time-resolved photon counting and direct photocurrent measurements. Upper curves in Fig. 5 show quenching of Eu related PL for EuF_3 after switching off the laser excitation. All the curves exhibit a very similar PL decay on the time scale being typical for Eu-related emission [25]. Red dotted lines in Fig. 5 illustrate fit of the experimental data with a single exponential decay

revealing a characteristic decay time of 0.33-0.34 ms. The bottom curve in Fig. 5 shows quenching of Eu related PL for the EuF_3 - diamond composite. Luminescence decay time 0.326-0.34 ms for EuF_3 particles embedded into the diamond films are in a good agreement with the results reported in [25] (0.325 ms). As one can see, this curve exhibits similar trend except for ~0.1 ms immediately after the excitation pulse. The increased rate of the PL quenching observed in the time range of 0-0.1 ms after an excitation pulse is apparently due to the contribution from the background emission which is characterized by the significantly lower decay time. The remaining part of the curve corresponds to the decay time of about 0.34 ms thus indicating the contribution from Eu-related emission.

4. Conclusions

We have prepared and characterized diamond-rare earth composite materials with EuF_3 NP embedded in microcrystalline CVD diamond films that exhibit photoluminescence emission at about 612 nm. We have developed a novel and very flexible technique that can be easily implemented for other rare-earth and alkaline-earth fluorides and/or oxides, so the latter species with unique optical and magnetic properties, including effective up-conversion and X-ray luminescence nanoparticles, can be easily incorporated into a polycrystalline diamond matrix. The luminescence decay of 612 nm line of 0.34 ms is similar for both EuF_3 powder and particles integrated into diamond films. Therefore, it is possible to produce diamond films with the tailored luminescence bands and life times of rare-earth elements of the choice. Our method can also be applied for the preparation of the multilayered composites with the same or different RE nanoparticles accommodated in their own layer(s) via repeated multiple-time diamond deposition. Alternatively, it is possible to seed a mixture of different RE species on the substrate surface to enhance the intensity and/or broaden spectral range of the PL emission to produce a multicolor light source. The luminescent properties of such composites can be further improved in order to reduce the background PL from non-diamond carbon by using a single crystal diamond substrate (instead of the polycrystalline one) to embed the RE NPs within the epitaxially grown diamond film. In addition, our method allows the use of such smaller lanthanide fluoride particles (as small as a few tens nanometers [41]), so this would enhance their localization within the diamond matrix. The encapsulation and overgrowth technique demonstrated in the present work can be regarded as a particular realization of a more general approach based on placing nano-or microparticles on diamond surface followed by epitaxial diamond deposition to fully or partially cover the particles and form a specific composite materials like diamond photonic crystal with buried silica opal structure [42], Li-doped diamond

film with Li_3N particles as the Li source [43], or bright X-ray beam monitors [8] with high thermal conductivity to operate at high intensity incident radiation fluxes. This promises a development of a wide variety of diamond-based functional composites with interesting optical, mechanical, magnetic properties.

Prime novelty statement

A novel type of diamond-based composite containing embedded luminescent europium trifluoride EuF_3 nanoparticles (NP) in the bulk is synthesized by MPCVD. The material exhibits bright photoluminescence in orange spectral range.

Acknowledgments

The part of this work on synthesis and characterization of EuF_3 nanopowders was supported by the Russian Foundation for Basic Research, grant No. 16-29-11784_ofi_m. The part of work on synthesis and characterization of diamond films and "Diamond-EuF_3" composites was supported by the Russian Science Foundation, grant No. 14-22-00243.

References

[1] S. Prawer, I. Aharonovich, Quantum Information Processing with Diamond: Principles and Applications, Elsevier, 2014.

[2] I. Aharonovich, E. Neu, Diamond Nanophotonics, Adv. Opt. Mater. 2 (2014) 911–928.

[3] J. Riedrich-Möller, C. Arend, C. Pauly, F. Mücklich, M. Fischer, S. Gsell, M. Schreck, C. Becher, Deterministic coupling of a single silicon-vacancy color center to a photonic crystal cavity in diamond, Nano Lett. 14 (2014) 5281–5287.

[4] L. Li, E.H. Chen, J. Zheng, S.L. Mouradian, F. Dolde, T. Schröder, S. Karaveli, M.L. Markham, D.J. Twichen, D. Englund, Efficient photon collection from a nitrogen vacancy center in a circular bullseye grating, Nano Lett. 15 (2015) 1493-1497.

[5] I. Aharonovich, S. Prawer, Fabrication strategies for diamond based ultra bright single photon sources, Diamond Relat.Mater. 19 (2010) 729-733.

[6] T.D. Merson, S. Castelletto, I. Aharonovich, A. Turbic, T.J. Kilpatrick, A.M. Turnley, Nanodiamonds with silicon vacancy defects for nontoxic photostable fluorescent labeling of neural precursor cells, Optics Lett. 38 (2013) 4170.

[7] T. Kudo, S. Takahashi, N. Nariyama, T. Hirono, T. Tachibana, H. Kitamura, Synchrotron radiation x-ray beam profile monitor using chemical vapor deposition diamond film, Rev. Sci. Instrum. 77 (2006) 123105.

[8] M. Degenhardt, G. Aprigliano, H. Schulte-Schrepping, U. Hahn, H.-J. Grabosch, E. Wörner, CVD diamond screens for photon beam imaging at PETRA III, J. Phys.: Conf. Ser. 425 (2013) 192022.

[9] R. Schirhagl, K. Chang, M. Loretz, C.L. Degen, Nitrogen-vacancy centers in diamond: nanoscale sensors for physics and biology, Ann. Rev. Phys. Chem. 65 (2014) 83–105.

[10] N. Felgen, B. Naydenov, S. Turner, F. Jelezko, J. P. Reithmaier, C. Popov, Incorporation and study of SiV centers in diamond nanopillars. Diamond Relat. Mater. 64 (2016) 64-69.

[11] V.G. Ralchenko, V.S. Sedov, A.A. Khomich, V.S. Krivobok, S.N. Nikolaev, S.S. Savin, I.I. Vlasov, V.I. Konov, Observation of the Ge-vacancy color center in microcrystalline diamond films, Bull. Lebedev Phys. Inst. 42 (2015) 165–168.

[12] E.A. Ekimov, S.G. Lyapin, K.N. Boldyrev, M.V. Kondrin, R. Khmelnitskiy, V.A. Gavva, T.V. Kotereva, M.N. Popova, Germanium–vacancy color center in isotopically enriched diamonds synthesized at high pressures, JETP Lett. 102 (2015) 701–706.

[13] I. Aharonovich, S. Castelletto, B.C. Johnson, J.C. McCallum, D.A. Simpson, A.D. Greentree, S. Prawer, Phys. Rev. B 81 (2010) 121201.

[14] S. Pezzagna, D. Rogalla, D. Wildanger, J. Meijer, A. Zaitsev, Creation and nature of optical centres in diamond for single-photon emission—overview and critical remarks, New J. Phys. 13 (2011) 035024.

[15] A. Bolshakov, V. Ralchenko, V. Sedov, A. Khomich, I. Vlasov, A. Khomich, N. Trofimov, V. Krivobok, S. Nikolaev, R. Khmelnitskii, V. Saraykin, Photoluminescence of SiV centers in single crystal CVD diamond *in situ* doped with Si from silane, Phys. Stat. Sol. (a) 212 (2015) 2525–2532.

[16] X. Huang, S. Han, W. Huang, X. Liu, Enhancing solar cell efficiency: the search for luminescent materials as spectral converters, Chem. Soc. Rev. 42 (2013) 173–201.

[17] Y.A. Rozhnova, A.A. Luginina, V.V. Voronov, R.P. Ermakov, S.V. Kuznetsov, A.V. Ryabova, D.V. Pominova, V.V. Arbenina, V.V. Osiko, P.P. Fedorov, White light luminophores based on $Yb^{3+}/Er^{3+}/Tm^{3+}$- coactivated strontium fluoride powders, MatChemPhys 148 (2014) 201–207.

[18] J. Hölsä, T. Laamanen, T. Laihinen, M. Lastusaari, L. Pihlgren, L.C. Rodrigues, White up-conversion luminescence of $NaYF_4$:Yb^{3+}, Pr^{3+}, Er^{3+}, Opt. Mater. 36 (2014) 1627–1630.

[19] C.C. Lin, R.-S. Liu, Advances in phosphors for light-emitting diodes, J. Phys. Chem. Lett. 2 (2011) 1268–1277.

[20] T. Yanagida, Study of rare-earth-doped scintillators, Opt. Mater. 35 (2013) 1987–1992.

[21] P.P. Fedorov, A.A. Luginina, A.I. Popov, Transparent oxyfluoride glass ceramics, J. Fluor. Chem. 172 (2015) 22–50.

[22] Y.Y. Hui, C.-L. Cheng, H.-C. Chang, Nanodiamonds for optical bioimaging, J. Physics D: Appl. Phys. 43 (2010) 374021.

[23] F. Wang, D. Banerjee, Y. Liu, X. Chen, X. Liu, Upconversion nanoparticles in biological labeling, imaging, and therapy, Analyst 135 (2010) 1839–1854.

[24] K. Tono, T. Togashi, Y. Inubushi, T. Sato, T. Katayama, K. Ogawa, H. Ohashi, H. Kimura, S. Takahashi, K. Takeshita, Beamline, experimental stations and photon beam diagnostics for the hard x-ray free electron laser of SACLA, New J. Phys. 15 (2013) 083035.

[25] A. Magyar, W. Hu, T. Shanley, M.E. Flatté, E. Hu, I. Aharonovich, Synthesis of luminescent europium defects in diamond, Nat. Comm. 5 (2014) 3523.

[26] B.P. Sobolev, The rare earth trifluorides: the high temperature chemistry of the rare earth trifluorides, Institut d'Estudis Catalans, 2000.

[27] P.P. Fedorov, A.A. Luginina, S.V. Kuznetsov, V.V. Osiko, Nanofluorides, J. Fluor. Chem. 132 (2011) 1012–1039.

[28] P.P. Fedorov, V.V. Osiko, S.V. Kuznetsov, O.V. Uvarov, M.N. Mayakova, D.S. Yasirkina, A.A. Ovsyannikova, V.K. Ivanov, Nucleation and growth of fluoride crystals by agglomeration of the nanoparticles, J.Crystal Growth, 401 (2014) 63–66.

[29] S.V. Kuznetsov, A.A. Ovsyannikova, E.A. Tupitsyna, D.S. Yasyrkina, V.V. Voronov, N.I. Batyrev, L.D. Iskhakova, V.V. Osiko, P.P. Fedorov, Phase formation in LaF_3-$NaGdF_4$, $NaGdF_4$-$NaLuF_4$, $NaYF_4$-$NaLuF_4$ systems: synthesis of powders by co-precipitation from aqueous solutions, J. Fluor. Chem. 161 (2014) 95–101.

[30] V. Sedov, V. Ralchenko, A.A. Khomich, I. Vlasov, A. Vul, S. Savin, A. Goryachev, V. Konov, Si-doped nano- and microcrystalline diamond films with controlled bright photoluminescence of silicon-vacancy color centers, Diam. Relat. Mater. 56 (2015) 23–28.

[31] P.P. Fedorov, M.N. Mayakova, S.V. Kuznetsov, V.V. Voronov, R.P. Ermakov, K.S. Samarina, A.I. Popov, V.V. Osiko, Co-precipitation of yttrium and barium fluorides from aqueous solutions, Mat. Res. Bull. 47 (2012) 1794–1799.

[32] V. S. Bagaev, V. S. Krivobok, S. N. Nikolaev, A. V. Novikov, E. E. Onishchenko, A. A. Pruchkina, Excitonic luminescence of SiGe/Si quantum wells δ-doped with boron, J. Appl. Phys. 117 (2015) 185705.

[33] D.P. Volanti, I.L. Rosa, E.C. Paris, C.A. Paskocimas, P.S. Pizani, J.A. Varela, E. Longo, The role of the Eu^{3+} ions in structure and photoluminescence properties of $SrBi_2Nb_2O_9$ powders, Opt. Mater. 31 (2009) 995–999.

[34] A.M. Zaitsev, Optical properties of diamond: a data handbook, Springer-Verlag, Berlin, Heidelberg, 2001.

[35] A. O'Riordan, E. O'Connor, S. Moynihan, X. Linares, R. Van Deun, P. Fias, P. Nockemann, K. Binnemans, G. Redmond, Narrow bandwidth red electroluminescence from solution-processed lanthanide-doped polymer thin films, Thin Solid Films 491 (2005) 264–269.

[36] W. Sun, J. Yu, R. Deng, Y. Rong, B. Fujimoto, C. Wu, H. Zhang, D.T. Chiu, Semiconducting polymer dots doped with europium complexes showing ultranarrow emission and long luminescence lifetime for time-gated cellular imaging, Angew. Chemie Int. Ed. 52(43) (2013) 11294-11297.

[37] T. Petzel, O. Greis, Uber phasenuntersuchungen und sattigungsdampfdruckmessungen an europium difluorid, Z. Anorg. Allg. Chemie 388 (1972) 137–157.

[38] S.M. Kaczmarek, T. Tsuboi, M. Ito, G. Boulon, G. Leniec, Optical study of Yb^{3+}/Yb^{2+} conversion in CaF_2 crystals, J. Phys.: Condens. Matter. 17 (2005) 3771.

[39] S.V. Stankus, R.A. Khairulin, K.M. Lyapunov, Phase transitions and thermal properties of gadolinium trifluoride, J. Alloys&Compounds, 290 (1999) 30-33.

[40] I.I. Vlasov, E. Goovaerts, V.G. Ralchenko, V.I. Konov, A.V. Khomich, M.V. Kanzyuba, Vibrational properties of nitrogen-doped ultrananocrystalline diamond films grown by microwave plasma CVD, Diam. Relat. Mater. 16 (2007) 2074–2077.

[41] E.M. Chan, G. Han, J.D. Goldberg, D.J. Gargas, A.D. Ostrowski, P.J. Schuck, B. E. Cohen, D. J. Milliron, Combinatorial discovery of lanthanide-doped nanocrystals with spectrally pure upconverted emission, Nano Lett. 12 (2012) 3839–3845.

[42] B. Dai, G.Shu, V. Ralchenko, A. Bolshakov, D. Sovyk, A.A. Khomich, V. Shershulin, K. Liu, J. Zhao, G. Gao L. Yang, P. Lei, J. Zhu, J. Han, 2D inverse periodic opal structures in single crystal diamond with incorporated silicon-vacancy color centers. Diam. Relat. Mater. (2016) online Oct 6.

[43] M.Z. Othman, P.W. May, N.A. Fox, P.J. Heard, Incorporation of lithium and nitrogen into CVD diamond thin films. Diam. Relat. Mater. 44 (2014) 1-7.

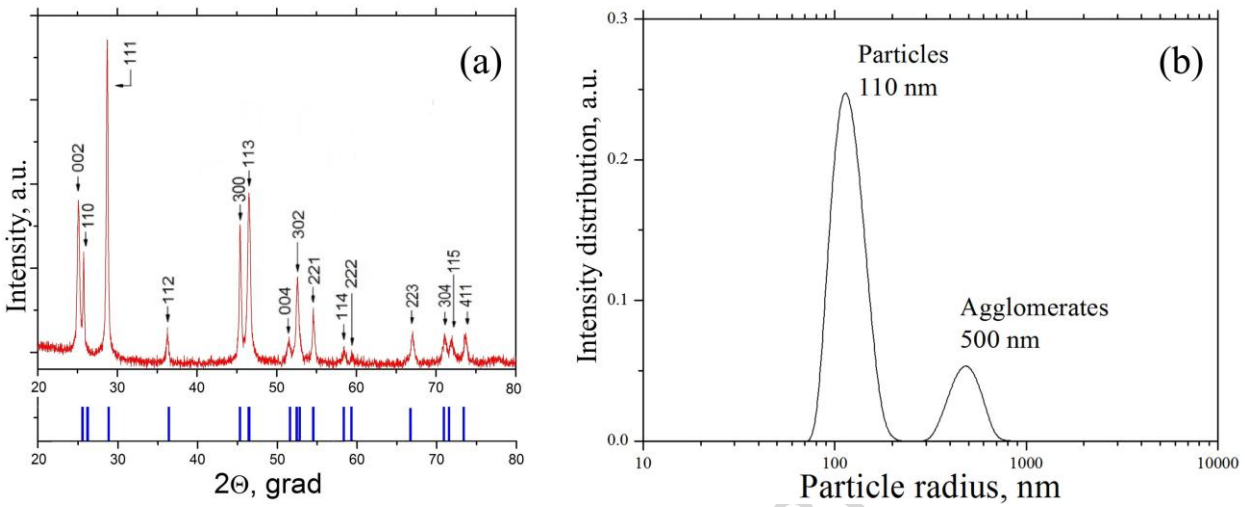

Fig. 1. X-ray diffraction pattern (a) of tysonite-type EuF_3 nano-powder (CuK_α radiation; literature data for the reflection angles are presented as blue bars below for comparison) and size distribution for EuF_3 nanoparticles in an aq. 0.1wt% slurry measured by dynamic light scattering (b).

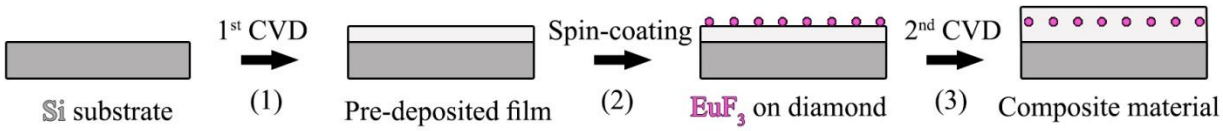

Fig. 2. The scheme of diamond composite preparation by imbedding EuF_3 nanoparticles between two microcrystalline diamond layers on the silicon substrate.

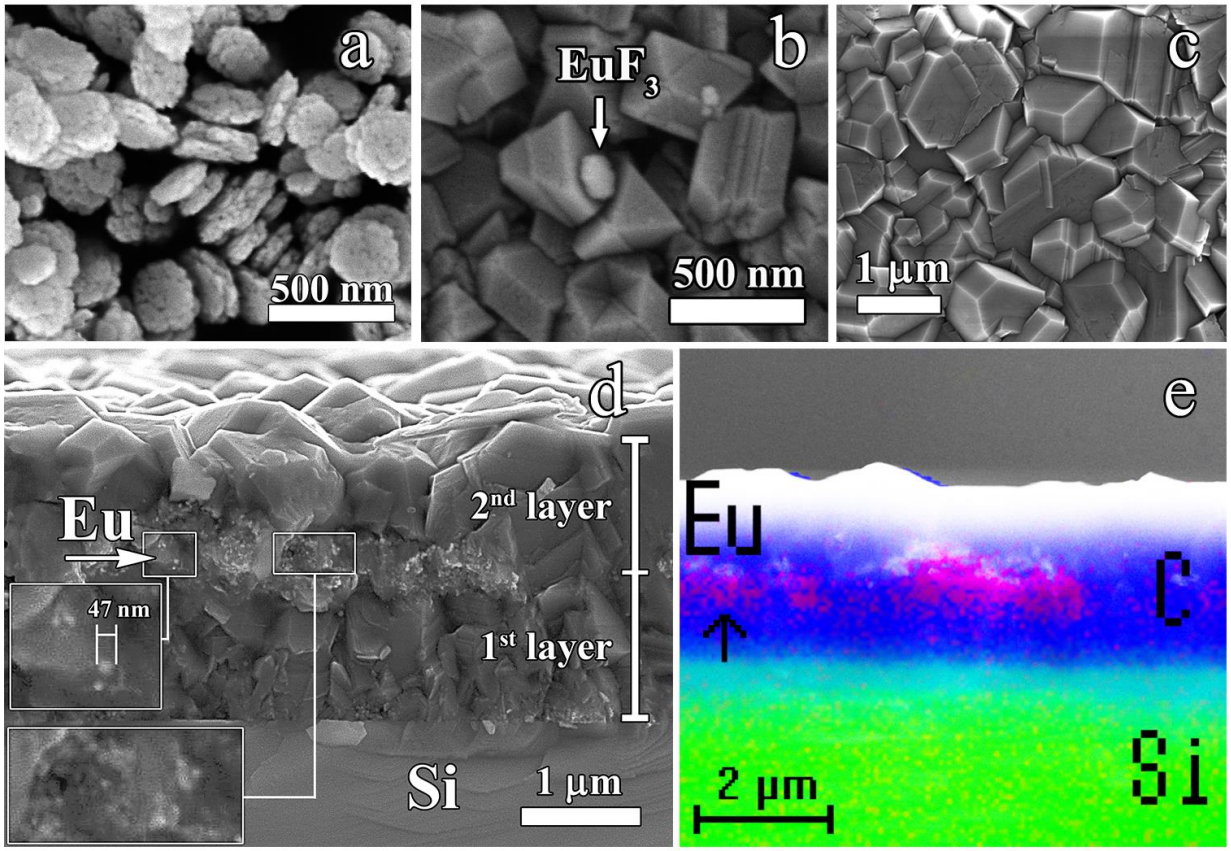

Fig. 3. SEM images (top views) of synthesized EuF_3 nano-powder (a), the seeded EuF_3 particles on a pre-deposited diamond film (b), and the surface of diamond film after the 2nd 40 min CVD growth on the top of EuF_3 particles (c). SEM image of the cross-section of the diamond film with imbedded EuF_3 particles in the middle of the film (d). EDX mapping of elements across the same cross-section (e): green layer – silicon, blue layer – carbon, purple dots – europium (also shown by the arrow).

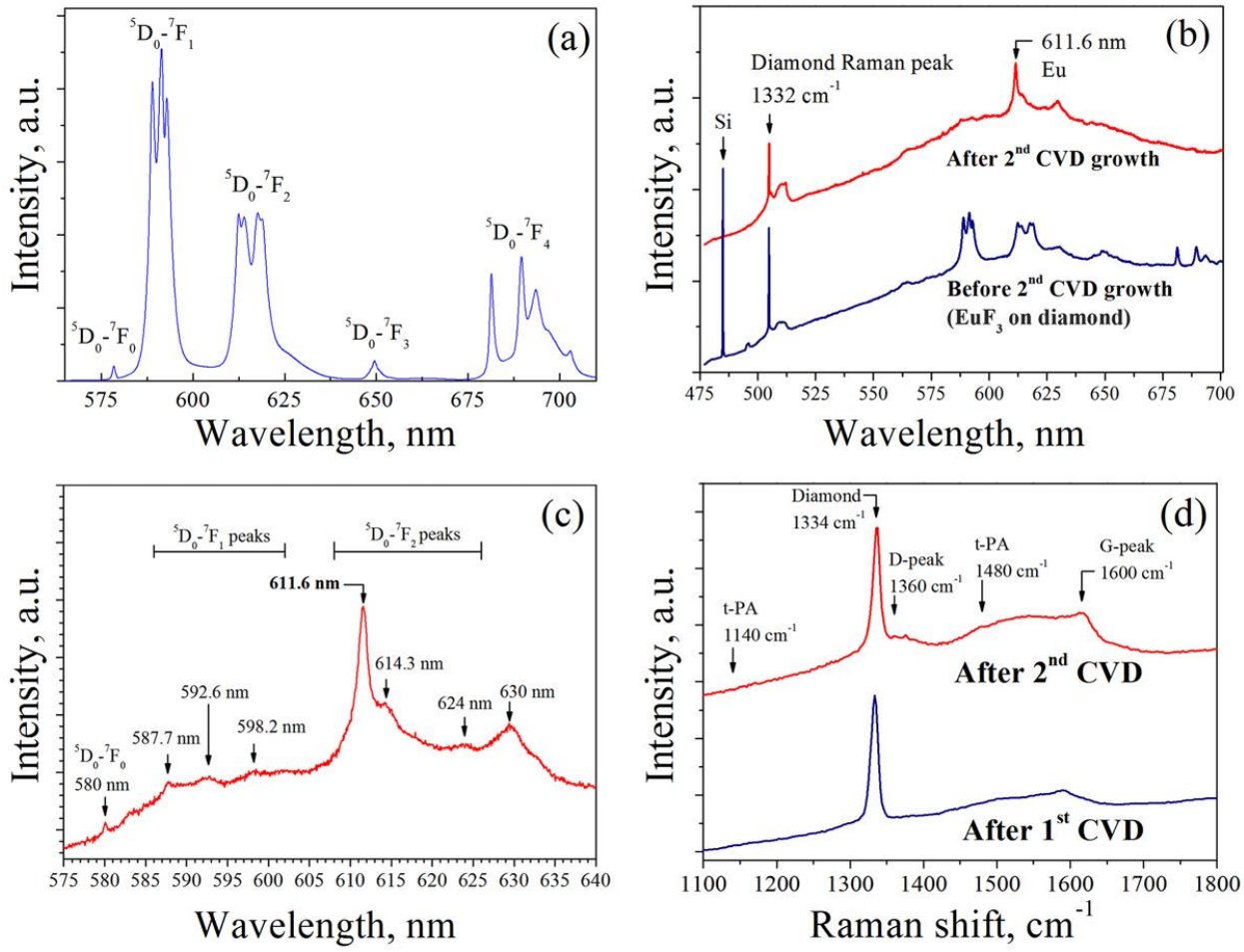

Fig. 4. PL spectrum of synthesized EuF_3 powder (λ_{exc} = 473 nm) (a). PL spectra for pre-deposited diamond film seeded with EuF_3 particles (bottom spectrum) and for the diamond film after 40 min CVD growth with embedded EuF_3 NP (top spectrum) (b). Broadening of the PL line between 575 nm and 675 nm was caused by NV^0 nitrogen-vacancy, NV^- defects and amorphous carbon impurity. The narrow lines at 486 nm and 505 nm are Raman peaks for silicon substrate and diamond, respectively. The strong 611.6 nm peak corresponds to the Eu^{+3} $^5D_0 \rightarrow {}^7F_2$ transition, while the appearance of the 630 nm line is caused by a specific CVD diamond defect. The high-resolution PL spectrum for the EuF_3 component in the composite film is shown in (c), while the Raman spectra for the pre-deposited diamond film (bottom) and the film containing EuF_3 NP after the 2nd 40 min growth (top) are in (d). All spectra were recorded at the 473 nm excitation wavelength at room temperature.

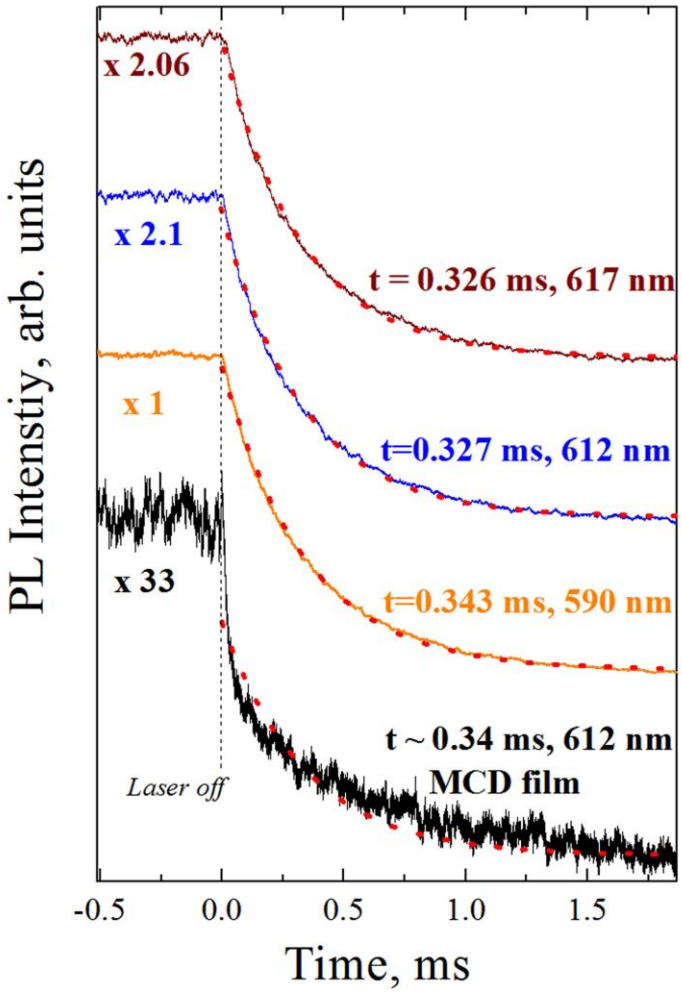

Fig. 5. PL decay of Eu related peak for EuF_3 powder (red – 617 nm, blue – 612 nm, orange – 590 nm) and for the EuF_3 - diamond composite (black line) after switching off the laser excitation. Red dotted lines show data fits with single exponential decay.

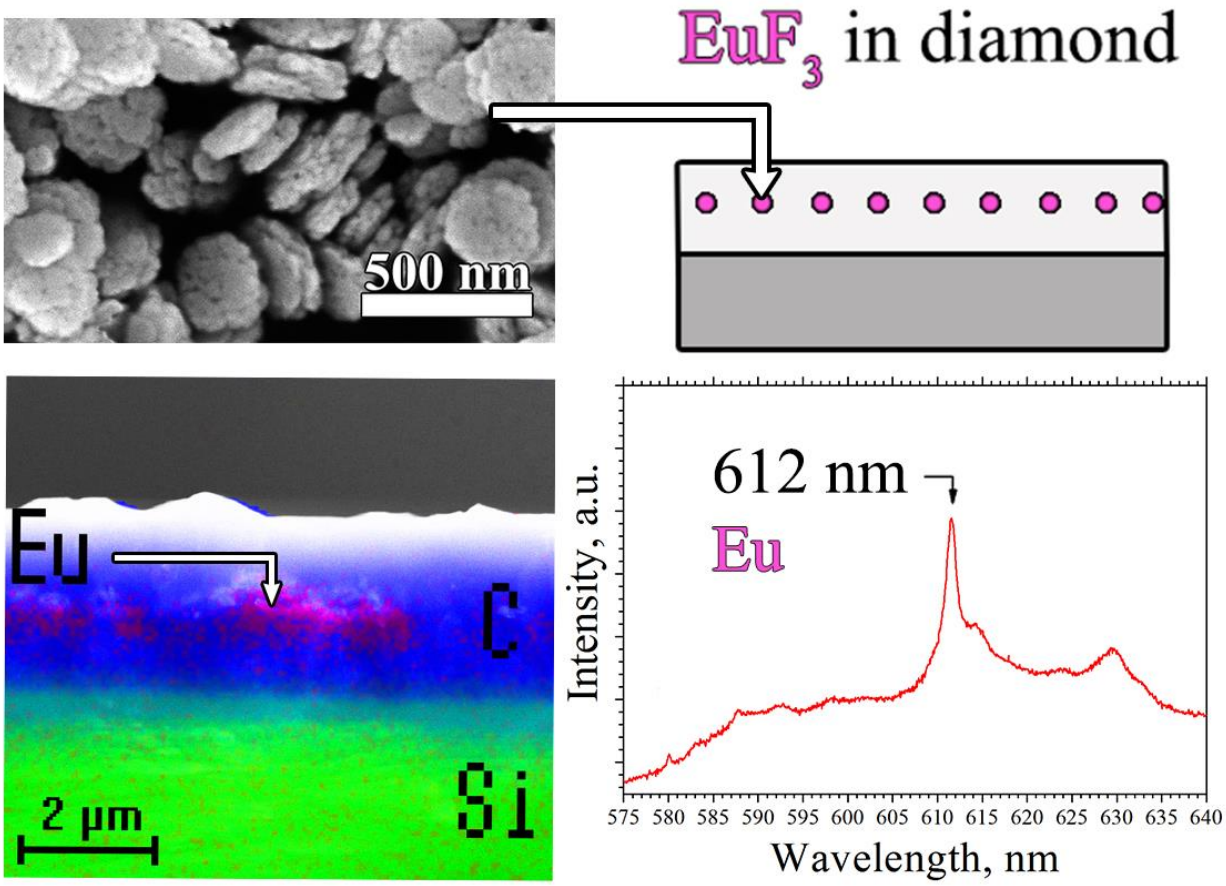

Graphical abstract

Highlights

1. Luminescent EuF_3 nanoparticles were integrated into diamond matrix using a CVD technique.
2. The diamond-EuF_3 nanocomposite shows narrow photoluminescence peak at 612 nm wavelength
3. The luminescence decay of 612 nm line is measured at 0.34 ms.